EXPERIMENTAL CELL RESEARCH 217, 410–418 (1995)

Intracellular Ionic Variations in the Apoptotic Death of L Cells by Inhibitors of Cell Cycle Progression

GIUSEPPE BARBIERO,*,[1] FEDERICA DURANTI,* GABRIELLA BONELLI,*
JOSEPH S. AMENTA,† AND FRANCESCO M. BACCINO*,‡

*Dipartimento di Medicina ed Oncologia Sperimentale, Università di Torino, corso Raffaello 30, 10125 Torino; †Department of Pathology, University of Pittsburgh School of Medicine, Pittsburgh, Pennsylvania 15260; and ‡Centro CNR di Immunogenetica ed Oncologia Sperimentale, Torino, Italy

Treatment with VP-16 (1–50 μM) or excess thymidine (5 mM) caused a block of L cells at different steps in their progression through the replicative cycle. The arrest was followed by an asynchronous process of cell death that conformed to criteria for apoptosis. Careful monitoring of this process in the whole cell population by flow cytometry showed a virtual absence of necrosis, an increase in side light scattering, followed by the occurrence of a population with subdiploid DNA fluorescence as well as reduced forward and side light scattering. The development of apoptosis required sufficient time and adequate ion gradients in the cells. By the combined use of flow cytometry and fluorescence microscopy data were obtained suggesting that (i) intracellular free Ca^{2+} and pH and/or their drug-induced alterations had to be adequately controlled for the apoptotic process to evolve; (ii) mitochondria were compromised earlier than the plasma membrane or lysosomes; and (iii) K^+ extrusion possibly played a role in the final loss of cell volume. Interfering with the control of ion gradients and/or their changes in drug-treated cells resulted in cell death by necrosis.

INTRODUCTION

Apoptosis is a mode of cell death, by condensation or shrinkage, that occurs in a variety of physiological and pathological situations. *In vitro* studies have demonstrated that cells may die by apoptosis if their progression through the replicative cycle is affected by the lack of adequate trophic support [1, 2]. Likewise, since the initial observations by Searle *et al.* [3], the apoptotic mode of cell death is now regarded as a final common pathway in the action of a variety of antiblastic agents [4–7], many of which interfere with cell cycle progression. Using monolayer cultures of L cells continuously exposed to excess thymidine [8] or the DNA topoisomerase inhibitor VP-16 [9], we have developed drug-induced models of cell death that share the basic features of apoptosis: chromatin condensation, elevation of transglutaminase activity, strong immunocytochemical reactivity of apoptosing cells for tissue transglutaminase, cell shrinkage, and formation of apoptotic bodies, though no internucleosomal DNA fragmentation detectable by agarose gel electrophoresis. In these models, cell detachment from the monolayer characterizes the concluding steps of the cell death process and is followed either by "secondary necrosis" of the apoptotic bodies (unpublished data) and/or by their homophagic disposal by viable cells in the monolayer [8, 10].

In addition to morphologic assessment, a number of other techniques have been applied to detect and quantify apoptosis in a cell population. Flow cytometric procedures have been extensively utilized in this regard (reviewed in [11]). These techniques permit rapid and detailed analysis of cell populations and can easily discriminate among viable, apoptotic, and necrotic subpopulations [12]. These features are particularly important when dealing with events that can be relatively rare and asynchronous, as is usually the case for apoptosis. Here we propose a flow cytometric method for the rapid monitoring of cell death obtained by inhibitors of cell cycle progression such as VP-16 (etoposide) or excess thymidine in L cell cultures. Although some precautions are needed when analyzing cells growing in monolayer, these models offer the opportunity to easily distinguish between early and late phases of the process (also see [13]).

Variations in intracellular free calcium ($[Ca^{2+}]_i$)[2] and

[1] To whom reprint requests should be addressed at Dipartimento di Medicina ed Oncologia Sperimentale, Sezione di Patologia Generale, Corso Raffaello, 30, 10125 Torino, Italy. Fax: 011-6707753. E-mail: in%"baccino@polito.it".

[2] Abbreviations used: $[Ca^{2+}]_i$, $[H^+]_i$, $[Na^+]_i$, $[K^+]_i$, intracellular free calcium, proton, sodium, and potassium concentrations, respectively; AM, acetoxymethyl ester; AO, acridine orange; BAPTA, 1,2-bis(*O*-aminophenoxy)ethane-*N*,*N*,*N*′,*N*′-tetraacetic acid] tetraacetoxymethyl ester; DMA, 5-(*N*,*N*-dimethyl)amiloride; D-MEM, Dulbecco's modified Eagle's medium; DMSO, dimethyl sulfoxide; EGTA, ethylene glycol bis(β-aminoethyl ether) *N*,*N*,*N*′,*N*′-tetraacetic acid; FCS, fetal calf serum; FITC, fluorescein isothiocyanate; FL, fluores-

0014-4827/95 $6.00

pH (pH_i) have been suggested as early events in the onset of apoptosis. In many, though not in all, studies an elevation of $[Ca^{2+}]_i$ has been reported to precede apoptosis induced by various agents [14–18]. The endonuclease activation involved in the internucleosomal cleavage of DNA has been suggested to be triggered by a $[Ca^{2+}]_i$ rise [14, 19] or, more recently, by a drop in pH_i [20, 21]. A prominent reduction in cell size characterizes the apoptotic mode of cell death [22, 23] and ions such as Na^+, K^+, and H^+ themselves are involved in fibroblast volume regulations [24]. Therefore, by the combined use of flow cytometry and fluorescence microscopy, we have monitored alterations in the intracellular concentrations of Ca^{2+}, H^+, Na^+, and K^+. The relevance of these changes to the development of apoptosis in the present models of drug-induced cell death is discussed.

MATERIALS AND METHODS

Cell culture and treatment. Mouse L cells were grown in D-MEM supplemented with 10% FCS, penicillin (100 units/ml), and streptomycin (100 μg/ml) and maintained at 37°C, in a humidified atmosphere of 5% CO_2 in air. Cultures were regularly checked for mycoplasma contamination by staining with the DNA-specific fluorochrome 4′-6-diamidine-2-phenylindole dihydrochloride (DAPI) (Boehringer, Mannheim, Germany) or by an enzyme immunoassay (Boehringer). Cells were seeded in 56-cm^2 petri dishes at a density of 12,000 cells/cm^2 and 24 h later (time 0) shifted to medium containing 0.1, 1, 5, 10, 20, 50, 100 μ*M* VP-16 or 5 m*M* thymidine. Experiments were extended for 3 to 7 days, with daily medium changes in order to ensure constant drug concentrations.

At each time point, cells from the monolayer were harvested by trypsinization and cells floating in the medium were collected by centrifugation. These were kept separate and resuspended in PBS. In both cases cell number and size were determined with an electronic cell counter (ZM, Coulter Electronics, Hialeah, FL). Cell viability, DNA, and protein content were evaluated on the whole population (monolayer plus medium). All other experiments were performed on cells from the monolayer alone.

DNA content. In view of the remarks about the subdiploid peak expressed by Darzynkiewicz *et al.* [11], a very strict protocol was used for cell fixation. Cell suspensions in PBS (10^6 cells/ml) were centrifuged at 0–2°C and the pellet was washed with PBS (at 0–4°C) and resuspended in ice-cold 70% ethanol for at least 30 min. After centrifugation cells were incubated at room temperature in the presence of DNase-free ribonuclease (Type 1-A) and PI at final concentrations of 0.4 and 0.18 mg/ml PBS, respectively. Fluorescence was measured using a FACScan flow cytometer (Becton–Dickinson, Mountain View, CA) equipped with a 488-nm light source (argon laser). Two filters were used to collect the red fluorescence due to PI staining the DNA, one transmitting at 585 nm with a bandwidth of 42 nm (FL2), the other transmitting above 620 nm (FL3). FL2 and FL3 were registered on a linear and on a logarithmic scale, respectively. Forward (FSC) and side (SSC) light scatter were simultaneously measured. The flow rate was set at about 200 cells/s and at least 10^4 cells were analyzed for each sample. Debris was excluded from analysis by appropriately raising FSC and FL3 thresholds to values selected experimentally. Data were recorded in a Hewlett Packard computer (HP 9000, Model 300), using CellFit software (Becton–Dickinson).

Biparametric flow cytometric analysis of DNA and protein. Cells fixed in ice-cold 70% ethanol were centrifuged and resuspended in PBS. FITC (1 μg/ml final concentration) was added to each sample. After 30 min at room temperature, DNase-free ribonuclease (0.4 mg/ml) and PI (0.18 mg/ml) were added and cells were gently mixed and kept for 15 min at room temperature before analysis. Green fluorescence due to protein labeling by FITC was collected by using a 525-nm filter with a 15-nm bandwidth (FL1), while PI fluorescence was measured as specified above. Adequate compensation was introduced to separate overlaps between FL1 and FL2, as established using Calibrate flow cytometer beads and Autocomp software (Becton–Dickinson).

Cell viability. Cell viability was assessed by three independent parameters, essentially as described elsewhere [25].

Plasma membrane integrity was checked by the PI exclusion test. Unfixed cells suspended in PBS (10^6/ml) were incubated with PI (10 μg/ml) and analyzed by flow cytometry. Cells excluding PI were considered either viable or apoptotic, while dead cells not excluding PI were considered either necrotic [25] or in the latest stages of apoptosis *in vitro* (corresponding to secondary necrosis according to Wyllie *et al.* [26]). In some experiments, monolayers were directly incubated with PI for 30 min and washed twice with PBS and then cells were detached by trypsinization and analyzed by flow cytometry.

The mitochondrial transmembrane potential was evaluated with R123. Cells resuspended in PBS were incubated for 30 min at 37°C with R123 (10 μg/ml, final concentration) and analyzed. Cells retaining R123 were considered either viable or apoptotic [25]. In three experiments cells were preincubated with R123 and then stained with PI as specified above and analyzed for both green (R123) and red (PI) fluorescence to compare PI exclusion and R123 retention.

The ability to maintain a low intralysosomal pH was evaluated by incubating monolayers in complete D-MEM in the presence of 4 μg/ml AO for 30 min at 37°C. Cells were then enzymatically detached, washed twice in PBS, and analyzed. The detection of red luminescence reflects a low lysosomal pH, which is typical of viable or apoptotic cells, whereas necrotic cells show green fluorescence only [25].

$[Ca^{2+}]_i$ measurements on single cells. Cells were loaded with fura-2/AM (2–4 μ*M* final concentration in complete D-MEM) by incubation for 20–30 min at room temperature (incubation at 37°C did not modify results), washed with PBS, and resuspended in 10 m*M* Hepes, pH 7.3, containing (in m*M*): 145 NaCl, 5 KCl, 1 $MgSO_4$, 10 glucose, 2 $CaCl_2$. $[Ca^{2+}]_i$ measurements were performed with an inverted microscope (Zeiss Axiovert, D) equipped with a photometer (Cairn Research, Ltd., UK) and devices to synchronize and decode the emitted light and to generate the F350/F380 ratio. The fluorescence ratio was calibrated vs $[Ca^{2+}]$ as described [27] using the equation

$$[Ca^{2+}] = K_d \times (R - R_{min})/(R_{max} - R) \times Sf_2/Sb_2. \quad (1)$$

A K_d of 225 n*M* was assumed for the Ca^{2+}–fura-2 interaction in the cytosolic environment. The measured values were: $R_{min} = 0.32 \pm 0.05$, $R_{max} = 6.82 \pm 2.4$, $Sf_2/Sb_2 = 9.42 \pm 0.68$ (means ± SD, $n = 6$).

$[Ca^{2+}]_i$ measurements by flow cytometry. Flow cytometric analysis of $[Ca^{2+}]_i$ was carried out using the Ca^{2+}-sensitive dye fluo-3/AM in association with the pH_i-sensitive dye snarf-1/AM. The two probes were directly added to the cultured medium at final 1 (fluo-3) and 0.2 (snarf-1) μ*M* concentrations, followed by 30 min incubation at 37°C. Cells were then detached by trypsinization and resuspended in the Hepes-buffered solution described above. On excitation at 488 nm fluo-3 emits at 525 nm (FL1), while snarf-1 is isoemissive at about 610 nm (FL3). As reported [28], the ratio of fluo-3/snarf-1 emissions is more sensitive to $[Ca^{2+}]_i$ oscillations than fluo-3 fluorescence alone. Chronys software (Becton–Dickinson) was used for data acquisition and analysis.

Calibration of the fluorescence vs $[Ca^{2+}]_i$, assuming a K_d of 400 n*M*

cence channel; FSC, forward light scatter; PBFI, potassium-binding benzofuran isophthalate; PBS, phosphate-buffered saline; pH_i, intracellular pH; PI, propidium iodide; R123, rhodamine 123; SBFI, sodium-binding benzofuran isophthalate; snarf-1, carboxyseminaphtorhodafluor-1; SSC, side light scatter; VP-16, etoposide.

for the Ca^{2+}–fluo-3 interaction in the cytosolic environment, was performed as described [29], based on the equation

$$[Ca^{2+}] = K_d \times (F - F_{min})/(F_{max} - F), \quad (2)$$

wherein F_{max} represents the maximum fluorescence obtained from cells permeabilized to Ca^{2+} with 2 μM ionomycin and F the fluorescence of the experimental samples. F_{min} was calculated from the equation

$$F_{min} = F_{max} - (F_{max} - F_{MnCl2}) \times 1.25 \quad (3)$$

as described [29]. F_{MnCl2} was obtained by adding 2 mM $MnCl_2$ to ionomycin-treated cells.

pH_i measurements by flow cytometry. Flow cytometric analysis of the intracellular pH (pH_i) was carried out with the pH-sensitive dye snarf-1/AM as described [30, 31]. Briefly, 1 mM snarf-1/AM in DMSO was added in the medium at a final concentration of 10 μM. Cells were incubated at 37°C for 30 min and then detached and resuspended in 25 mM Hepes, pH 7.3, containing (in mM): 140 NaCl, 5.4 KCl, 0.8 $MgSO_4$, 5 glucose, 2 $CaCl_2$ and immediately analyzed. In some experiments, this solution was replaced with one containing bicarbonate (in mM: 43 $NaHCO_3$, 110 NaCl, 5.4 KCl, 2 $CaCl_2$, 0.8 $MgSO_4$, 25 Hepes, pH 7.3).

A calibration curve was obtained according to the equation [30]

$$[H^+]_i = [H^+]_e \times [K^+]_i/[K^+]_e. \quad (4)$$

Control cells were suspended in the above described buffer containing both the proton ionophore nigericin and higher KCl in order to achieve a K^+ concentration ($[K^+]_e$) approximately equal to the intracellular one ($[K^+]_i$). In the presence of nigericin, the pH_i reflects the extracellular pH (pH_e). At 488 nm excitation, snarf-1 emits at 585 (FL2) and 620 nm (FL3). The FL2/FL3 ratio measured on cells in the presence of nigericin at varying pH_e was used to relate histogram channel number to pH_i.

$[Na^+]_i$ and $[K^+]_i$ measurements on single cells. SBFI/AM and PBFI/AM were dissolved in DMSO (5 mg/ml) and stored at −20°C. Immediately before use, each solution was mixed with an equal volume of Pluronic F-127 (20% in DMSO) and added to cell suspensions (final probe concentration: 10 μM); these were incubated for 60 min at 37°C and then washed with PBS and resuspended in 10 Hepes, pH 7.3, containing (in mM): 145 NaCl, 5 KCl, 1 $MgSO_4$, 10 glucose, 2 $CaCl_2$.

SBFI and PBFI fluorescence was measured [32] with the same equipment used for $[Ca^{2+}]_i$ measurement on single cells. Instrumentation setup was independently adjusted for SBFI and PBFI. SBFI (or PBFI) fluorescence as a function of $[Na^+]_i$ (or $[K^+]_i$) was calibrated *in situ* with cells bathed by media of known $[Na^+]$ (or $[K^+]$) prepared by mixing different amounts of two solutions of equal ionic strength: one Na^+-free, containing 100 mM potassium gluconate and 30 mM KCl, the other containing 100 sodium gluconate and 30 mM NaCl. Both solutions contained 10 mM Hepes, 2 mM $CaCl_2$, and 1 mM $MgSO_4$. The 350/380-nm fluorescence ratio was determined before and 3 min after addition gramicidin D (1–2 μM final concentration) which equilibrated Na_i^+ and Na_e^+ as well as K_i^+ and K_e^+. Gramicidin D (1 μM final concentration) and valinomycin (2 μM final concentration) were used for PBFI calibration only.

Chemicals. D-MEM and FCS were purchased from Biochrom (Berlin, D); calmidazolium, DMA, DMSO, DNase-free ribonuclease (Type 1-A), FITC, gramicidin D, ionomycin, ouabain, penicillin, PI, R123, streptomycin, thymidine, trypsin, valinomycin, and VP-16 from Sigma (St. Louis, MO); AO, fura-2, fluo-3, snarf-1, nigericin, SBFI, PBFI, and Pluronic F-127 from Molecular Probes (Eugene, OR).

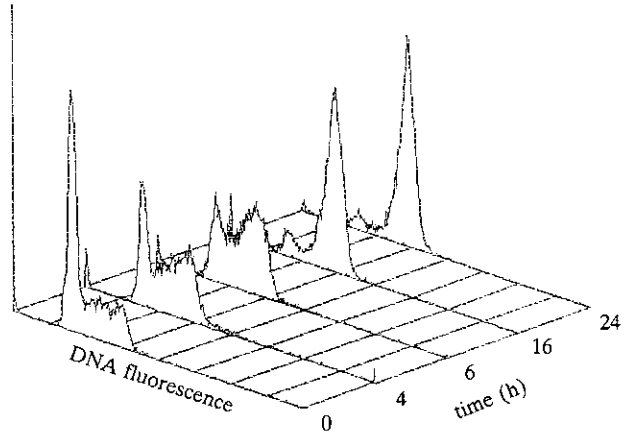

FIG. 1. DNA distribution in L cells from monolayers exposed to continuous treatment with 1 μM VP-16 for different times. Cells were progressively blocked in late S and G2–M phases of the cell cycle.

RESULTS

Previous reports had shown that 5 mM thymidine [8] and 10 μM VP-16 [9] not only totally inhibited L cell growth, as estimated from the number of cells or the total cell protein in the monolayer, but also induced, after a 24-h lag, an asynchronous process of cell death manifesting the morphological features of apoptosis and associated with cell detachment from the monolayer.

Cell Cycle Arrest and Cell Death

When exponentially growing L cell cultures were continuously exposed to various concentrations of VP-16 for up to 7 days, virtually all cells on 1–50 μM VP-16 were blocked in the late S and G2–M phases by 24 h (Fig. 1), in agreement with other findings on various cell types [7, 21]; in surviving cells in the monolayer such blockade may persist for up to 7 days. On 5 mM thymidine, L cells were arrested in the G1–S phases by 24 h (not shown; cf. [33]). The protein/DNA ratio in L cells was increased after 24 h on 5 mM thymidine and after 48 h on 1–50 μM VP-16, indicating that protein and DNA accumulation were unbalanced (Fig. 2); the latter change can be largely ascribed to the divergence between protein synthesis, which remained well active, and DNA replication, largely ceased [8, 9]. Except for these findings relating to the different mechanisms leading to growth arrest, most further observations on cells treated with thymidine or VP-16, particularly at 10 μM concentration, were quite comparable; therefore, the following sections will mostly illustrate only results obtained with 10 μM VP-16.

Forward light scatter, a parameter indicative of cell volume, and side light scatter, indicative of "cellular density," were monitored by flow cytometry in L cells treated with VP-16 (Fig. 3) or thymidine (not shown).

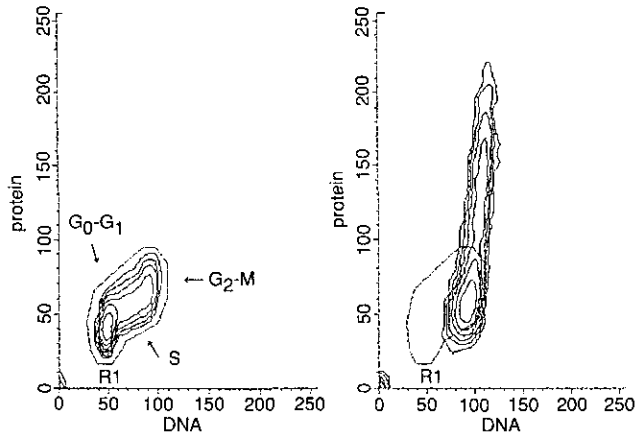

FIG. 2. Unbalanced protein/DNA ratio induced in L cells by VP-16. Controls (left panel) and cells exposed to 5 μM VP-16 (right panel) at Day 2. An earlier increase of the ratio was observed on 5 mM thymidine (not shown; cf. [8]) likely reflecting the different time course of DNA synthesis inhibition.

Both FSC and SSC progressively increased until 24 h of treatment, then remained approximately unchanged the next day, and eventually decreased at Day 3, when a large subpopulation of apoptotic bodies was present, characterized by low FSC, very low SSC, as well as by subdiploid PI fluorescence. By impedance measurements [8], the diameter of these apoptotic bodies was found to be 7–10 μm, much less than the average diameter of t_0 cells (14–16 μm) or than that of S- and G2/M-arrested cells.

Cleavage of nuclear DNA into multiples of 180–200 bp, as detectable by agarose gel electrophoresis ("DNA ladder"), is usually regarded as a key feature of apoptosis (reviewed in [34]). It has been shown that flow cytometry can detect the emergence of a population characterized by a subdiploid DNA fluorescence, slightly lower than that in the G0/G1 peak, and that this correlates with the occurrence of the DNA ladder [35, 36]. In the present experiments, a prominent "subdiploid" population, with reduced FSC (cf. Figs. 3 and 4), developed in L cell cultures treated with VP-16. On 5–10 μM VP-16 (Fig. 4), this population was prominent in the medium by Day 1 and also in the monolayer by Day 3. Such a subdiploid population, however, was characterized by a DNA fluorescence less than 10% of 2n and thus in the cytogram was much more "distal," with respect to the G1 peak, than the usual "proximal" subdiploid peak [35, 36]. By electron microscopy, typical apoptotic bodies were observed in the cell population harvested from the monolayer; moreover, the subdiploid population recovered from the medium was mostly formed by typical apoptotic bodies, a substantial part of which showed clear signs of secondary necrosis (unpublished observations). Since cells with an apparent DNA content intermediate between the distal peak and the G0–G1 level were unfrequent, it should be inferred that the DNA degradation process was extremely rapid, in keeping with the results of a more detailed study on this issue (J. S. Amenta, M. J. Sargus, F. Duranti, G. Barbiero, F. M. Baccino, and G. Bonelli, manuscript in preparation).

Viability Tests

Three viability tests, PI exclusion and R123 or AO retention, were performed by flow cytometry on L cell cultures exposed to VP-16 or thymidine, examining cells in both monolayers and media. Dead cells neither excluding PI nor retaining AO were almost undetectable with 1–5 μM VP-16 and occurred only to a very limited extent with 10–50 μM VP-16 or 5 mM thymidine. By contrast, dead cells were prominent with 100 μM VP-16, from 6 h on, yet no typical apoptotic cells could be detected at this drug concentration. Figure 5 illustrates the results obtained with 10 μM VP-16. At any experimental time point, although in the medium the proportion of PI-excluding or AO-retaining cells was much lower, most cells in the monolayer were able both to exclude PI and to retain AO (≥95% until Day 3); the

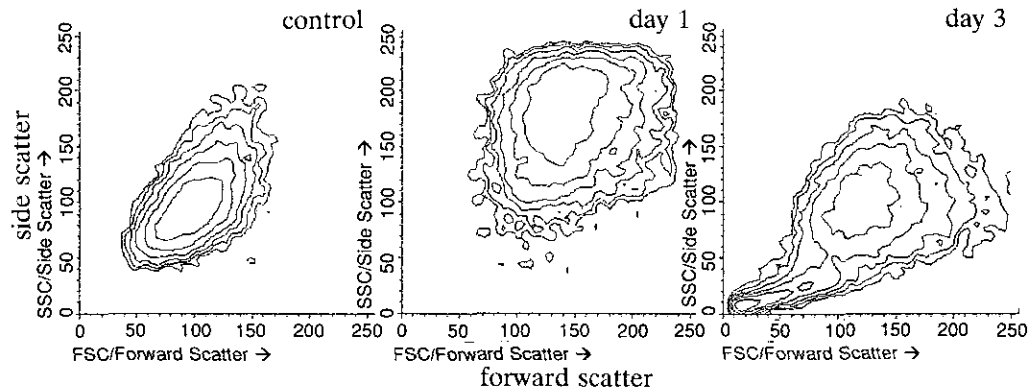

FIG. 3. Side light scatter (SSC) vs forward light scatter (FSC). Control (Day 1) and treated L cells (10 μM VP-16) at Day 1 and Day 3.

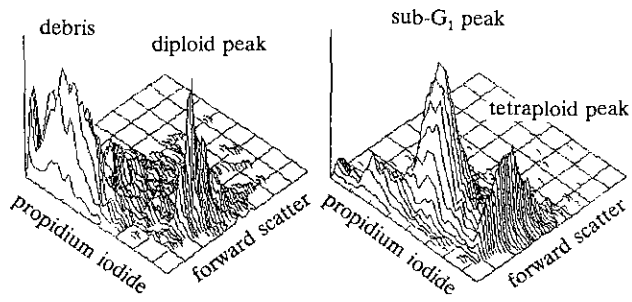

FIG. 4. Forward light scatter vs log PI fluorescence in ethanol-fixed L cells (monolayer plus medium). Left panel, control cells, showing a peak of debris. Right panel, cells exposed to 10 μM VP-16 for 4 days; FSC was gated to exclude debris, thus showing that the sub-G1 peak was clearly distinct. Cells in this sub-G1 population were only a little smaller (8–14 μm diameter) than controls (12–16 μm diameter), while their PI fluorescence was about 5% of the G2–M value.

latter figures are entirely consistent with previous data showing that at any time of the treatment with 10 μM VP-16 or 5 mM thymidine only $\leq$2% of the cells in the monolayer were permeable to trypan blue and thus should be considered "dead" by this routine viability test [8, 9].

By contrast, the proportion of cells that retained R123 was definitely lower both in the monolayer (83% at Day 3 and 70% at Day 4 on 10 μM VP-16) and in the medium (23% at Day 4). Plotting the time course of the changes for the three viability tests in the monolayers or in the whole population (monolayer plus medium, Fig. 5b) shows that mitochondrial functionality was compromised earlier than integrity of both the plasma membrane and the lysosomal system, which changed in parallel. Thus, cells that were still able to exclude PI and had a functional lysosomal pump had lost the ability to maintain a mitochondrial transmembrane potential.

Intracellular Free Calcium

$[Ca^{2+}]_i$ has been reported to increase in many experimental models of apoptosis [14, 15, 17, 18]. In cultures exposed to various concentrations of VP-16 or 5 mM thymidine, $[Ca^{2+}]_i$ was monitored both on individual L cells by fluorescence microscopy and on cell populations by flow cytometry. With 1–50 μM VP-16 or 5 mM thymidine we could not detect any rapid elevation of the $[Ca^{2+}]_i$, in keeping with previous reports on other cell lines [20, 21, 37–40]. Rather, the $[Ca^{2+}]_i$ slowly increased from 97 nM to approximately 150 nM in the initial 6 h and then returned to basal levels at 24 h (Fig. 6).

We next studied whether blocking this slow increase in $[Ca^{2+}]_i$ would prevent cell death. Cells pretreated for 30 min with 20 μM BAPTA-AM, an intracellular chelator, were exposed to the drugs, either 1–10 μM VP-16 or 5 mM thymidine. During the first hour the $[Ca^{2+}]_i$ remained at or below the lower level of detectability (approximately 35 nM), then gradually increased, reaching the basal level (approximately 100 nM) after 3 h of drug treatment. No further variation was observed until 16–24 h, when a large part of the population became necrotic, as indicated by the above viability tests (Fig. 7). Necrosis rather than apoptosis also developed after 16–24 h of exposure to VP-16 or thymidine when L cells were treated with 10 μM calmidazolium, a calmodulin inhibitor, over the initial 6-h period. Control L cells exposed to either agent were unaffected (data not shown).

Intracellular pH

A shift in pH_i, down to 6.6–6.8, has been reported in human promyelocytic HL-60 cells undergoing apoptosis

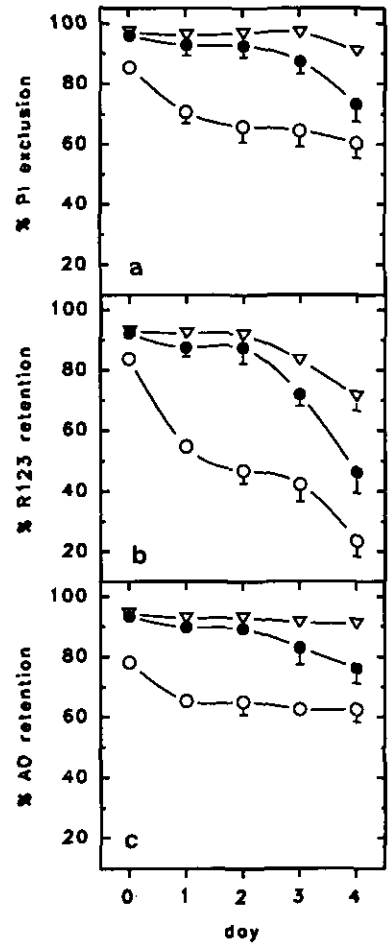

FIG. 5. Viability tests on L cells treated with 10 μM VP-16. Plasma membrane integrity (PI exclusion), mitochondrial transmembrane potential (R123 retention), and lysosomal pH (AO retention) evaluated on monolayer (▽), medium (○), or total (●) cells. Percentages on the ordinates represent the fraction of drug-treated cells whose fluorescence was within an area gating selected to include $\geq$98% of control cells. Data are means of five experiments, vertical bars represent SD (not shown when smaller than symbols). The percentage of cells in the monolayer amounted to 94% at Day 0, 89% at Day 1, 87% at Day 2, 71% at Day 3, and 48% at Day 4.

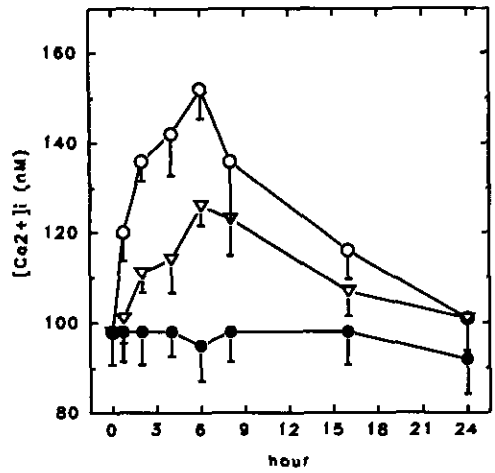

FIG. 6. Intracellular free calcium ($[Ca^{2+}]_i$). Measurements on single control cells (●) and cells exposed to 1 μM VP-16 (○) or 5 mM thymidine (▽). Data are means of ≥30 cells examined in seven separate experiments; vertical bars represent SD.

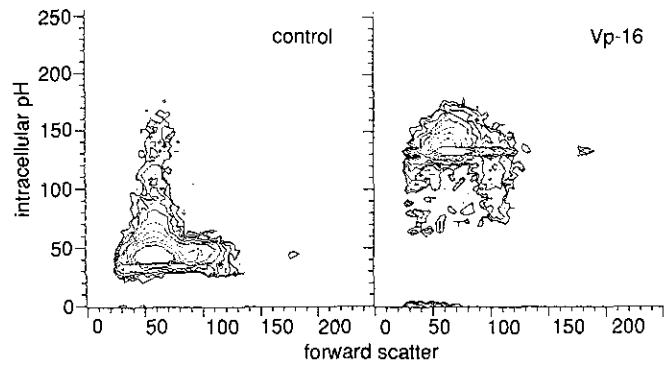

FIG. 8. Effect of 10 μM VP-16 on pH_i in L cells (24 h). Snarf-1 fluorescence ratio (585/620 nm, excitation 488 nm) vs FSC. An increase in the ratio corresponds to a decrease in pH_i.

by VP-16 and proposed as the triggering event for the internucleosomal DNA fragmentation [21]. In L cells treated with 1–50 μM VP-16 or 5 mM thymidine the pH_i, measured by flow cytometry, progressively and homogeneously declined, maximally by 0.2–0.4 units at 24 h (Fig. 8), and gradually rose during the next 48 h, reaching a basal value of 7.3 by 72 h (Fig. 9). To exclude the possibility that the pH_i drop resulted from a rapid loss of intracellular HCO_3^- in the course of the flow analysis, we repeated this experiment substituting the Hepes-buffered medium with a bicarbonate-containing solution. A comparable pH_i drop was observed in three experiments with this buffer. In further experiments 100 μM DMA, an inhibitor of the Na^+–H^+ exchanger, was applied to L cells at h 6 or 24 of the VP-16 treatment (the time of initial and of maximal inflection of the pH_i) to investigate whether such exchanger played a role in the pH_i recovery. However, by 48 h these cells underwent extensive necrotic death, whereas in control cultures DMA caused necrosis in less than 10% of cells.

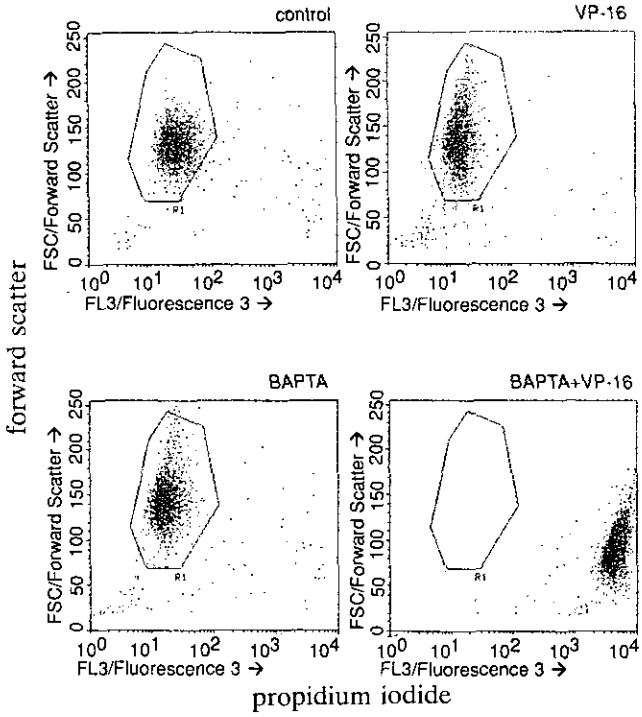

FIG. 7. Effect of chelation of intracellular Ca^{2+} on plasma membrane integrity. Control cells (left panels) and cells treated with VP-16 (right panels) at Day 1. Cells preloaded with BAPTA for 30 min before t_0 (lower panels).

Intracellular Sodium and Potassium

Since cell volume changes were prominent in these drug-treated L cells, we examined whether other ions involved in volume regulations, such as Na^+ and K^+, underwent significant alterations. As measured by fluorescence microscopy with the probe SBFI on single L cells in the monolayer, $[Na^+]_i$ increased from an average

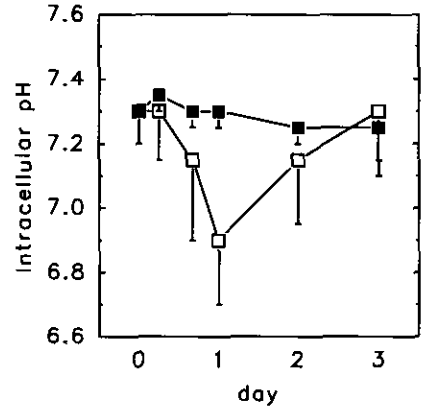

FIG. 9. pH_i variations in L cells treated with 1 μM VP-16. Control (■) and experimental (□) cells. Flow cytometric data are means of at least five experiments, vertical bars represent SD. Difference statistically significant at Day 1 ($P < 0.01$ by Student's t test).

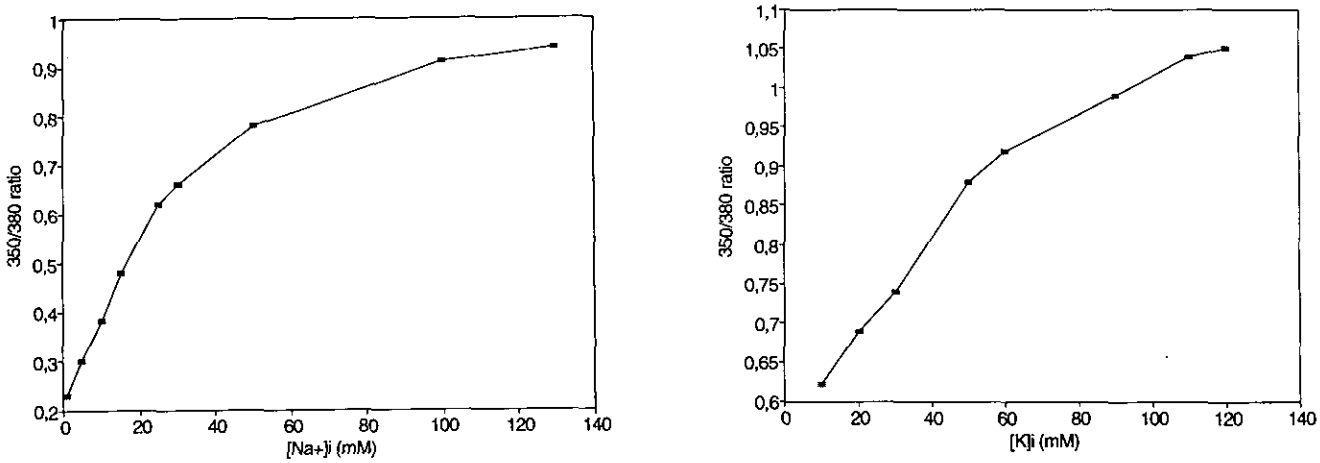

FIG. 10. *In situ* calibration curves for SBFI (left panel) and PBFI (right panel). See Materials and Methods for details.

15 m*M* at t_0 to a steady value of approximately 30 m*M*, attained by the second day of treatment with 10 μM VP-16. On Day 3, $[Na^+]_i$ was 30 m*M* in 94% of cells. Very high $[Na^+]_i$ ($\geq$110 m*M*) was found in 6% of the VP-16-treated cells, but this was similar to the percentage found in control cultures (5%) and also close to the percentage of cells that did not exclude PI in both control and treated cultures.

Because the affinity of the PBFI probe for K^+ was only 1.5-fold higher than that for Na^+ [41] (Fig. 10), measurements of $[K^+]_i$ in the presence of substantial $[Na^+]_i$ changes were precluded. In the present models, however, the $[Na^+]_i$ did not appreciably change after Day 2; therefore, any difference measured after this time using PBFI should primarily reflect $[K^+]_i$ changes. At Day 3 (Fig. 11) the $[K^+]_i$ was approximately 110 m*M* in control cells. In VP-16 treated cells a marked reduction in $[K^+]_i$ ($\leq$50 m*M*) was found in 18% of the cells examined in the monolayer. Assuming that cell loading or leakage did not differ for SBFI and PBFI, the difference between the frequency of cells with low $[K^+]_i$ (18%) and the frequency of cells with high $[Na^+]_i$ (6%) should be accounted for by cells having both low $[Na^+]_i$ (30 m*M*) and low $[K^+]_i$ (<50 m*M*). Such a pattern was likely related to the decrease in cell size characteristic of apoptosis.

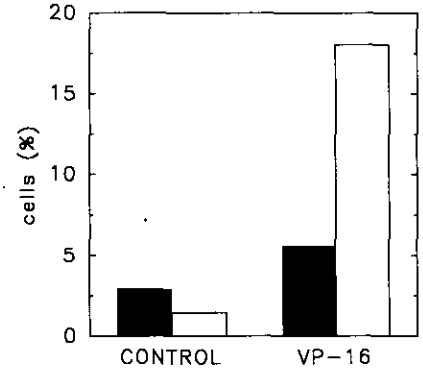

FIG. 11. Intracellular Na^+ and K^+ in L cells treated with 10 μM VP-16 for 3 days. $[Na^+]_i$ and $[K^+]_i$ measured on single cells in the monolayer with SBFI (n = 205 for controls, n = 214 for VP-16) and PBFI (n = 222 for controls, n = 233 for VP-16), respectively. Data represent percentages of cells with $[Na^+]_i \geq 30$ m*M* (black columns) or with $[K^+]_i \leq 50$ m*M* (open columns). The difference (12%) between such percentages for VP-16-treated cells should be accounted for by cells with $[Na^+]_i \leq 30$ m*M* and $[K^+]_i \leq 50$ m*M*.

DISCUSSION

When exponentially growing monolayers of L cells were continuously exposed to VP-16 (1–50 μM) or thymidine (5 m*M*), cells progressively accumulated in the G2–M or G1–S phases, respectively, of the cell cycle until by 24 h a complete growth arrest was achieved. Thereafter, cell death developed as an asynchronous process, manifesting with the morphological features of apoptosis [8, 9]. The overall fraction of dead cells measured by flow cytometry in the whole cell population (monolayer plus medium) shifted from 4% (t_0) to about 29% (Day 3). These figures show the accumulation of dead cells in the cultures, reflecting rates of cell death as well as rates of disposal of dead cells by homophagy [10] or of their disintegration into fragments (unpublished data). For a comparison, the fractional rates of cell loss, as estimated from DNA radioactivity decay in the monolayer, amounted to 0.53/day on thymidine [8] and 0.57/day on 10 μM VP-16 [9].

The present data show that at any time during the different treatments the vast majority of cells in the monolayer were "viable," as evaluated by current viability tests, though many cells had already entered the early stages of the apoptotic process. By contrast, the cells released into the medium corresponded to advanced stages of the process or even to postapoptotic changes [9] of the kind referred to as "secondary necrosis" [26]. Thus, detachment from the substrate gener-

ally marked some well-defined step in the apoptotic process. Moreover, the present data show that the current viability tests often are not interchangeable, do not clearly distinguish between apoptotic and viable cells, nor discriminate necrosis from the postapoptotic changes ("secondary necrosis") as occurring in tissue cultures.

In the present models the mitochondrial failure (loss of R123 retention) distinctly preceded the loss of integrity of both the plasma membrane and lysosomes. This finding would indicate that functional mitochondria were not required in the concluding phases of the apoptotic process. Of interest in this regard are recent observations showing that apoptosis in various cell types, L929 cells included, can be elicited by inhibitors of the mitochondrial electron transport chain, such as rotenone and antimycin, or by oligomycin, a mitochondrial ATP-synthetase inhibitor [42].

The onset of the apoptotic changes in L cells was preceded by an elevation of the SSC of cells, in agreement with previous observations on apoptosing thymocytes [23], as well as by a slow but steady increase of $[Ca^{2+}]_i$ in the initial 6 h of treatment. Cells then recovered basal levels of $[Ca^{2+}]_i$ at 24 h, when the cell cycle arrest was complete. Moreover, when cell death subsequently became manifest, no further $[Ca^{2+}]_i$ alteration could be detected in cells in the monolayer or in the medium.

Lowering $[Ca^{2+}]_i$ by the use of an intracellular chelator (BAPTA) can prevent the occurrence of apoptosis in HL-60 cells treated with VP-16 [39]. Consistently, since calmodulin mediates most Ca^{2+}-dependent reactions, calmodulin inhibitors can prevent apoptosis [43, 44]. In the present experiments L cells treated with VP-16 or thymidine combined with either BAPTA or calmidazolium resulted in extensive necrotic cell death. These observations suggest that Ca^{2+} played a role in the coordinated sequence of events underlying apoptotic death of L cells and that with lack of an adequate $[Ca^{2+}]_i$ the death process appeared to default to a necrotic mode.

In L cells exposed to 1–50 μM VP-16 or 5 mM thymidine the pH_i downshift, largely coincident with the growth arrest, likely reflected the cell cycle blockade [30]. Blocking the Na^+–H^+ exchanger with DMA both prevented L cells from recovering basal pH_i levels (7.3) at 48 h and caused necrotic death in a substantial fraction of them (approximately 50%). These observations indicate that the Na^+–H^+ exchanger was actively involved in the pH_i recovery in such cells and further suggest that this activity was required for cell to progress into the apoptotic process, whereas blocking the exchanger unbalanced the ionic fluxes to the point of precipitating cells into necrotic (colloidoosmotic) lysis.

Both an increase in cell size, associated with the cell cycle blockade, and a subsequent decrease in size, associated with apoptosis, have been observed in the present models. Changes in $[K^+]_i$ were evaluated with regard to the final cell shrinkage. In spite of the limitations of the technique we used to measure $[K^+]_i$, a significant fraction of cells in the monolayer after 3 days of treatment were characterized by a strongly decreased $[K^+]_i$, although still maintaining an appreciable barrier function of the plasma membrane (PI exclusion, only moderate increase of $[Na^+]$, PBFI retention). The presence at Day 3 of cells with $[Na^+]_i$ about 30 mM and $[K^+]_i$ <50 mM is similar to observations on dense SS (homozygous) red blood cells in sickle cell anemia. Classical studies [45–47] demonstrated that this subpopulation is characterized by slightly increased $[Na^+]_i$ and markedly decreased $[K^+]_i$, correlating with changes in size and morphology of erythrocytes. One possible explanation may be that cell swelling activates a KCl symport resulting in a cell volume decrease driven by the K^+ gradient [24, 48, 49]. Therefore, although the intracellular Cl^- was not measured in the present work, the present data are not incompatible with the hypothesis that an active K^+ extrusion took part in the shrinkage of L cells.

Concluding Remarks

The present observations, derived from the study of two different drug treatments, show that blockade of L cells at different steps in their progression through the replicative cycle is followed by a process of cell death that conforms to criteria for apoptosis. Careful monitoring of this process in the whole cell population by flow cytometric techniques provided data consistent with morphological and biochemical investigations [8, 9] and also permitted easy discrimination between the necrotic and the apoptotic modes of cell death. In spite of the different initial effects of the two drugs, the process elicited by excess thymidine or VP-16 appeared basically similar by all the parameters investigated. This would suggest that the blockade in the cell cycle or some related event(s) somehow signaled the apoptotic process in cells. By the combined use of flow cytometry and fluorescence microscopy, data were obtained suggesting that (i) a certain level of $[Ca^{2+}]_i$, though not necessarily its observed slight increase, was required for the apoptotic death; (ii) mitochondria were compromised earlier than the plasma membrane or lysosomes; and (iii) K^+ extrusion possibly played a role in the final loss of cell volume. Taken together our data suggest that inhibition of L cell progression through the replicative cycle by thymidine or VP-16 leads to a slow and asynchronous cell death process, the development of which by the apoptotic mode requires time and specific intracellular ionic conditions. When these conditions are not fulfilled, cells may, by default, manifest only plasma membrane failure, i.e., necrotic death. We ignore whether the present observations might also imply that in the present models these two modes of cell death were alternative [50]. Further work is needed to evaluate such a possibility.

The authors gratefully acknowledge Drs. Davide Lovisolo, Emanuele Albano, and Renzo Levi for critical reading of the manuscript, Dr. Alex Pelizzola for assistance in interpreting DNA flow cytometry data, Drs. Giorgio Bellomo, Francesco Di Virgilio, and Tullio Pozzan for valuable discussions, and Drs. Paola Bergnolo, Enrica Fara, and Enrica Pazé for technical assistance. This study was supported by grants from the Associazione Italiana per la Ricerca sul Cancro, Milano, the Consiglio Nazionale delle Ricerche (Special Project A.C.R.O.), Roma, and the Ministero per l'Università e la Ricerca Scientifica e Tecnologica, Roma.

REFERENCES

1. Rodriguez-Tarduchy, G., Collins, M., and Lopez-Rivas, A. (1990) *EMBO J.* **9,** 2997–3002.
2. Evan, G. I., Wyllie, A. H., Gilbert, C. S., Littlewood, T. D., Land, H., Brooks, M., Waters, C. M., Penn, L. Z., and Hancock, D. C. (1992) *Cell* **69,** 119–128.
3. Searle, J., Lawson, T. A., Abbott, P. J., Harmon, B., and Kerr, J. F. R. (1975) *J. Pathol.* **116,** 129–138.
4. Dive, C., Evans, C. A., and Whetton, A. D. (1992) *Semin. Cancer Biol.* **3,** 417–427.
5. Hickman, J. A. (1992) *Cancer Metastasis Rev.* **11,** 121–139.
6. Lowe, S. W., Ruley, H. E., Jacks, T., and Housman, D. E. (1993) *Cell* **74,** 957–967.
7. Gorczyca, W., Gong, J., Ardelt, B., Traganos, F., and Darzynkiewicz, Z. (1993) *Cancer Res.* **53,** 3186–3192.
8. Amenta, J. S., Sargus, M. J., Baccino, F. M., Sacchi, C., and Bonelli, G. (1993) *In Vitro Cell Dev. Biol.* **29A,** 855–861.
9. Bonelli, G., Sacchi, C., Barbiero, G., Duranti, F., Goglio, G., Piacentini, M., Amenta, J. S., and Baccino, F. (1993) *in* General Pathology and Pathophysiology of Aging (Bergamini, L., Ed.), pp. 105–110, Wichtig, Milan.
10. Amenta, J. S., and Baccino, F. M. (1989) *Cell Biol. Rev.* **21,** 401–422.
11. Darzynkiewicz, Z., Bruno, S., Del Bino, G., Gorczyca, Z., Hotz, M. A., Lassota, P., and Traganos, F. (1992) *Cytometry* **13,** 795–808.
12. Dive, C., Gregory, C. D., Phipps, D. J., Evans, D. L., Milner, A. E., and Wyllie, A. H. (1992) *Biochim. Biophys. Acta* **1133,** 275–285.
13. Ormerod, M. G., O'Neill, C. F., Robertson, D., and Harrap, K. R. (1994) *Exp. Cell Res.* **211,** 231–237.
14. McConkey, D. J., Nicotera, P., Hartzell, P., Bellomo, G., Wyllie, A. H., and Orrenius, S. (1989) *Arch. Biochem. Biophys.* **269,** 365–370.
15. Ojcius, D. M., Zychlinsky, A., Zheng, L. M., Ding, E., and Young, J. (1991) *Exp. Cell Res.* **197,** 43–49.
16. Bellomo, G., Perotti, M., Taddei, F., Mirabelli, F., Finardi, G., Nicotera, P., and Orrenius, S. (1992) *Cancer Res.* **52,** 1342–1346.
17. Zhivotovsky, B., Nicotera, P., Bellomo, G., Hanson, K., and Orrenius, S. (1993) *Exp. Cell Res.* **207,** 163–170.
18. Jiang, S., Chow, S. C., Nicotera, P., and Orrenius, S. (1994) *Exp. Cell Res.* **212,** 84–92.
19. Arends, M. J., Morris, R. G., and Wyllie, A. H. (1990) *Am. J. Pathol.* **136,** 593–608.
20. Barry, M. A., and Eastman, A. (1993) *Biochem. Biophys. Res. Commun.* **186,** 782–789.
21. Barry, M. A., Reynolds, J. E., and Eastman, A. (1993) *Cancer Res.* **53,** 2349–2357.
22. Cohen, J. J. (1991) *Adv. Immunol.* **50,** 55–85.
23. Swat, W., Ignatowicz, L., and Kisielow, P. (1991) *J. Immunol. Methods* **137,** 79–87.
24. Wöll, E., Ritter, M., Scholz, W., Haussinger, D., and Lang, F. (1993) *FEBS Lett.* **322,** 261–265.
25. Del Bino, G., Lassota, P., and Darzynkiewicz, Z. (1991) *Exp. Cell Res.* **193,** 27–35.
26. Wyllie, A. H., Kerr, J. F. R., and Currie, A. R. (1980) *Int. Rev. Cytol.* **68,** 251–306.
27. Grynkiewicz, G., Poenie, M., and Tsien, R. Y. (1985) *J. Biol. Chem.* **260,** 3440–3450.
28. Rijkers, G. T., Justement, L. B., Griffioen, A. W., and Cambier, J. C. (1990) *Cytometry* **11,** 923–927.
29. Vandenberghe, P. A., and Ceuppens, J. L. (1990) *J. Immunol. Methods* **127,** 197–205.
30. Musgrove, E., Seaman, M., and Hedley, D. (1987) *Exp. Cell Res.* **172,** 67–75.
31. Van Erp, P. E. J., Jansen, M. J. J. M., De Jongh, G. J., Boezeman, J. B. M., and Schalkwijk, J. (1991) *Cytometry* **12,** 127–132.
32. Borin, M., and Siffert, W. (1990) *J. Biol. Chem.* **265,** 19543–19550.
33. Naus, G. J., Trucco, G., Sargus, M. J., and Amenta, J. S. (1994) *In Vitro Cell Dev. Biol.* **30A,** 15–16.
34. Peitsch, M. C., Mannherz, H. G., and Tschopp, J. (1994) *Trends Cell. Biol.* **4,** 37–41.
35. Nicoletti, I., Migliorati, G., Pagliacci, M. C., Grignani, F., and Riccardi, C. (1991) *J. Immunol. Methods* **139,** 271–279.
36. Telford, W. G., King, L. E., and Fraker, P. J. (1991) *Cell. Proliferation* **24,** 447–459.
37. Alnemri, E. S., and Litwack, G. (1990) *J. Biol. Chem.* **265,** 17323–17333.
38. Lennon, D. V., Kilfeather, S. A., Hallett, M. B., Campbell, A. K., and Cotter, T. G. (1992) *Clin. Exp. Immunol.* **87,** 465–471.
39. Yoshida, A., Ueda, T., Takauji, R., Liu, Y. P., Fukushima, T., Inuzuka, M., and Nakamura, T. (1993) *Biochem. Biophys. Res. Commun.* **196,** 927–934.
40. Treves, S., Trentini, P. L., Ascanelli, M., Bucci, G., and Di Virgilio, F. (1994) *Exp. Cell Res.* **211,** 339–343.
41. Minta, A., and Tsien, R. Y. (1989) *J. Biol. Chem.* **264,** 19449–19457.
42. Wolvetang, E. J., Johnson, K. L., Krauer, K., Ralph, S. J., and Linnane, A. W. (1994) *FEBS Lett.* **339,** 40–44.
43. Lee, S., Christakos, S., and Small, M. B. (1993) *Current Opinion Cell Biol.* **5,** 286–291.
44. Shaposhnikova, V. V., Dobrovinskaya, O. R., Gukovskaya, A. S., Trepakova, E. S., and Korystov, Y. N. (1993) *FEBS Lett.* **324,** 274–276.
45. Kurantsin-Mills, J., Kudo, M., and Koso Addae, S. (1974) *Clin. Sci. Mol. Med.* **46,** 679–692.
46. Clark, M. R., Unger, R. C., and Shohet, S. B. (1978) *Blood* **51,** 1169–1178.
47. Glader, B. E., Lux, S. E., Muller-Soyano, A., Platt, O. S., Propper, R. P., and Nathan, D. G. (1978) *Br. J. Haematol.* **40,** 527–532.
48. Jennings, M. L., and Schulz, R. K. (1990) *Am. J. Physiol.* **259,** C960–C967.
49. Lauf, P. K., Bauer, J., Adragna, N. C., Fujise, H., Zade-Oppen, A. M. M., Ryu, K. H., and Delpire, E. (1992) *Am. J. Physiol.* **263,** C917–C932.
50. Arends, M. J., McGregor, A. H., and Wyllie, A. H. *Am. J. Pathol.* **144,** 1045–1057.

Received August 10, 1994
Revised version received November 18, 1994